

Short communication

Effect of ultrasonic treatment and temperature on nanocrystalline TiO₂

D.H. Kim, H.W. Ryu, J.H. Moon, J. Kim*

Department of Materials Science and Engineering, Chonnam National University, 300 Yongbong-dong, Buk-ku, Gwangju 500-757, South Korea

Received 8 August 2005; received in revised form 15 December 2005; accepted 20 December 2005
Available online 8 February 2006

Abstract

Nanocrystalline TiO₂ particles were precipitated from the ethanol solution of titanium isopropoxide (Ti(O-*i*Pr)₄) and H₂O₂ by refluxing at 80 °C for 48 h. The obtained particles were filtered and dried at 100 °C for 12 h. The dried powder itself, the sample with heating at 400 °C, and the sample with ultrasonically treating were prepared to investigate the effects of post treatments on materials characteristics and electrochemical properties of nanocrystalline TiO₂. The X-ray diffraction patterns of all of the samples were fitted well to the anatase phase. The field emission-TEM image of as-prepared sample shows a uniform spherical morphology with 5 nm particle size and the sample heated at 400 °C shows slightly increased particle size of about 10 nm while maintaining spherical shape. The sample treated with ultrasonic for 5 h or more at room temperature shows high aspect ratio particle shape with an average diameter of 5 nm and a length of 20 nm. According to the results of the electrochemical testing, as-prepared sample, the sample heated at 400 °C for 3 h, and the sample treated with ultrasonic show initial capacities of 270, 310 and 340 mAh g⁻¹, respectively.

© 2006 Elsevier B.V. All rights reserved.

Keywords: Nanocrystalline; Particles; TiO₂; Morphology; Ultrasonic

1. Introduction

The demand for high energy density, high capacity and high-rate capability rechargeable batteries has stimulated the search for new materials [1]. Various systems have been developed for lithium ion batteries employing graphite as an anode [2–5]. However, the graphite anode has some disadvantages such as its initial loss of capacity, structural deformation and electrical disconnection. For example, when manganese-based cathodes are combined with graphite anodes, manganese reacts with electrolyte, LiPF₆, and is dissolved to form MnF. This phenomenon has been proved to cause the degradation of electrochemical properties. To circumvent these problems, a various class of anode materials, transition metal oxides (MoO₂, SnO₂, Ta₂O₅, NiO, CoO, CuO, FeO and Li₄Ti₅O₁₂), have been investigated [6–9].

Among these, titanium oxide has been found to be one of the good candidates as an anode for lithium ion batteries with advantages of a high capacity, low cost and non-toxicity. Huang et al. have showed a low capacity of 50 mAh g⁻¹ for nano-size TiO₂ [8]. Natarajan et al. have reported amorphous, nanocrystalline and crystalline TiO₂ phases obtained by aqueous peroxy route show a maximum reversible discharge capacity of 140 mAh g⁻¹ [10]. M. Hibino et al. have reported amorphous titanium oxide electrode for high-rate discharge and charge with a capacity of 120 mA g⁻¹ under a high current density such as 10 A g⁻¹ [11]. Zhou et al. have reported TiO₂ nanotube for anode material with a capacity of 184 mA g⁻¹ in the voltage range of 1–3 V [12]. Abraham and co-workers have synthesized micrometer-sized Li₄Ti₅O₁₂ at 800 °C using solid-state reaction with a capacity of 140 mAh g⁻¹ [13,14].

We have investigated the influence of ultrasonic and heat treatments on nanocrystalline TiO₂ and its electrochemical properties as an anode material in the lithium ion batteries. The objective was to obtain a better understanding of the synthesis conditions on characteristics of nanocrystalline TiO₂ so as to achieve desirable electrochemical performances.

* Corresponding author. Tel.: +82 62 530 1703; fax: +82 62 530 1699.
E-mail address: jaekook@chonnam.ac.kr (J. Kim).

2. Experiment

A 0.01 M TTIP (titaniumtetraisopropoxide) was added to ethanol of 100 mL. Subsequently, 30% H₂O₂ was added in the solution. The molar ratio of H₂O₂ and Ti(O-*i*Pr)₄ was fixed at 12:1. The solution was heated at 80 °C for 48 h in a round bottom flask attached with refluxing condenser. In order to remove ethanol and adsorbed organic substances, the solution containing nanocrystalline precipitates was washed with 200 mL of acetone several times. The particles were filtered and dried in an oven at 100 °C for 12 h to evaporate impurities. The obtained particles were heated at 400 °C for 3 h. The washed solution was treated with ultrasonic for 5 h or more at room temperature. The obtained particles were separated by filtering using ceramic membrane funnels. Subsequently, the filtered particles were dried in an oven at 100 °C for 12 h. The samples with or without ultrasonic treatment, and the sample heat-treated at 400 °C were therefore prepared and characterized to understand their physical properties and electrochemical performances.

The crystalline nature of the obtained nanocrystalline TiO₂ was characterized by X-ray diffraction. The particle morphology, size and chemical properties were observed by field emission-TEM and FT-IR, respectively. The discharge cycling of nanocrystalline TiO₂ was carried out with lithium metal as the reference electrode. Cells were fabricated is based on the following configuration: Li metal(-)/electrolyte/TiO₂(+) with a liquid electrolyte (1 M LiPF₆ in EC/DMC) and TAB (Teflonated Acethylene Black) binder.

3. Results and discussion

Fig. 1 shows the XRD patterns (a) of as-prepared sample, (b) the sample heated at 400 °C for 3 h, and (c) the sample treated with ultrasonic, respectively. All of the diffrac-

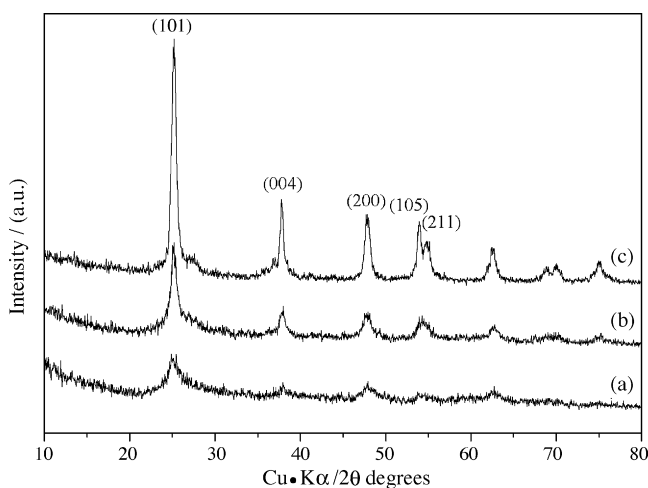


Fig. 1. XRD patterns of (a) the as-prepared sample, (b) the sample heated at 400 °C for 3 h, and (c) the sample treated with ultrasonic, which are assigned to anatase phase TiO₂.

tion peaks in these patterns are assigned to anatase phase TiO₂. When the as-prepared sample was heated at 400 °C for 3 h, the widths of the XRD peaks became narrower compare with as-prepared sample, as shown in Fig. 1(b). The sample treated with ultrasonic shows that the widths of the XRD peaks even narrower compare with both of as-prepared sample and the sample heated at 400 °C for 3 h, as shown in Fig. 1(c). It indicates that there was an increase in crystalline size with ultrasonic treatment, eventhough the sample was not undergone any high temperature heat treatment. The primary particle size, *d*, was calculated from the X-ray line width using the Scherrer formula $d = 0.9\lambda / \beta_{1/2} \cos \theta$ where λ is X-ray wavelenth, $\beta_{1/2}$ the corrected width of the main diffraction peak at half-height and θ the diffraction angle. The *d* values of the as-prepared sample, the sample heated at 400 °C for 3 h, and the sample treated with ultrasonic was 10, 12 and 15 nm, respectively. The XRD analysis reveals that the sample heated 400 °C for 3 h or the sample treated with ultrasonic lead to the high crystallinity and increased crystalline size. And also, we could say in the XRD analysis that the high nanocrystalline TiO₂ can be obtained at low temperature just by using ultrasonic treatment without any heat treatments.

Fig. 2 shows field emission-TEM images of the nanocrystalline TiO₂. The as-prepared sample shows aggregated nanocrystalline TiO₂ particles. The size of primary particles is about 5 nm. The sample heated at 400 °C for 3 h shows increased primary particle size of 10 nm. These results indicate that crystalline size of the obtained TiO₂ increased from 5 to 10 nm as the heating temperature increased from 100 to 400 °C. The sample treated with ultrasonic shows high aspect ratio particle shape morphology with an average diameter of 5 nm and a length of 20 nm. It gives three times higher intensity than the sample heated at 400 °C for 3 h in XRD analysis. It indicates that the sample treated with ultrasonic has a high crystallinity than the sample heated at 400 °C for 3 h. The XRD and TEM analysis reveals that this ultrasonic treatment will be an effective process to improve the crystallinities of nanoparticles in solution media.

Fig. 3 shows the FT-IR spectra of as-prepared sample, the sample heat-treated at 400 °C for 3 h, and the sample treated with ultrasonic. The absorption spectrum from 3000 to 3600 cm⁻¹ in Fig. 3 are assigned to the stretching vibration of the hydrogen-bonded OH groups of the adsorbed water, while the spectrum in 1600 and 1380 cm⁻¹ can be assigned to the bending vibration of absorbed H₂O and the stretching vibration of CO₃²⁻ ion, respectively. This may be due to the adsorbed species on sample surface. For the reason, we can observe relatively stronger spectrum from the smaller particle-sized samples. The absorption region at 912 and 717 cm⁻¹ in Fig. 3 can be, respectively, assigned to the stretching vibration of the O–O bond and the Ti–O bond in the Ti–O–O–H bond of the peroxy titanate Ti(OH)₃(OOH). The above results indicate that the Ti-peroxy compounds as impurity do not exist in samples. Therefore, we reached a conclusion the samples are consist of pure nanocrystalline anatase TiO₂.

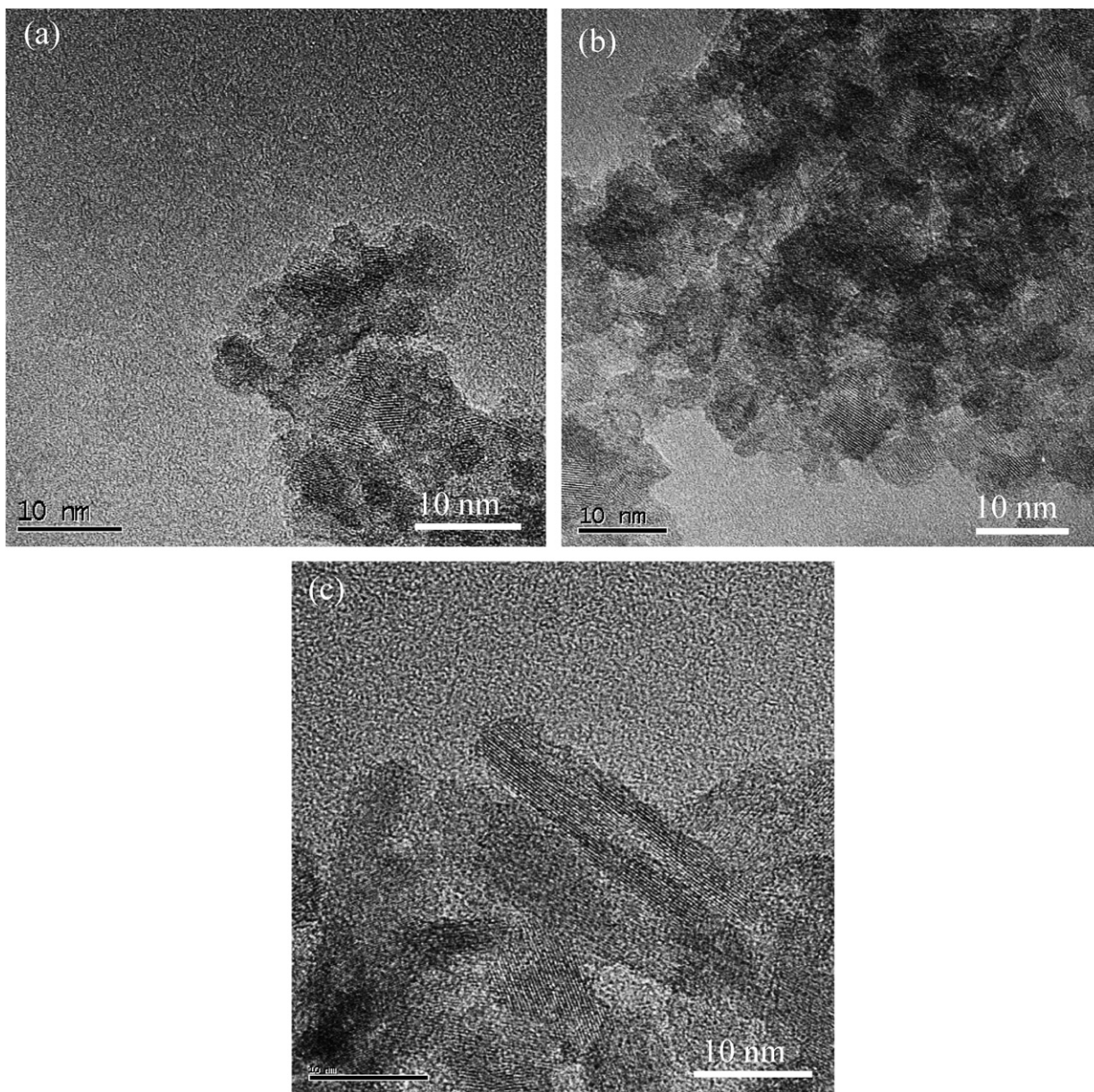


Fig. 2. Field emission transmission-electron microscopy (FE-TEM) images of (a) the as-prepared sample, (b) the sample heated at 400 °C for 3 h, and (c) the sample with ultrasonic treatment.

Fig. 4 shows the initial discharge profiles at various (0.05, 0.1, 0.2 and 0.4 mA cm⁻²) current densities in the voltage range of 2.5–0.5 V. Fig. 4 (a), as-prepared sample, shows a continuous sloping discharge profile, since it consists of very fine nanoparticles with short range ordering. The as-prepared sample shows a poor rate capability at various (0.05, 0.1, 0.2 and 0.4 mA cm⁻²) current densities, although it gives a good initial capacity of 270 mAh g⁻¹ at the 0.05 mA cm⁻² current density. The sample heated at 400 °C for 3 h in Fig. 4(b) shows a plateau in the voltage range of 1.5–1.7 V, due to its relatively long range ordering compared with the as-prepared sample with initial capacity of 305 mAh g⁻¹ at current density 0.05 mA cm⁻². Initial capacities are 305, 204, 175 and

168 mAh g⁻¹ at various current densities of 0.05, 0.1, 0.2 and 0.4 mA cm⁻², respectively. It exhibits a better rate capability than the as-prepared sample. The sample treated with ultrasonic in Fig. 4(c) shows that plateau pre-eminently in the voltage of about 1.7 V with initial capacity of 340 mAh g⁻¹ at current density 0.05 mA cm⁻². Initial capacities are 340, 328, 258 and 121 mAh g⁻¹ at current densities of 0.05, 0.1, 0.2 and 0.4 mA cm⁻². Although this sample treated with ultrasonic shows a larger initial capacity, the rate capability is worse than the sample heated at 400 °C for 3 h. These results suggest, at least partially, that the spherical particle morphology with size of around 10 nm could help to attain a better rate capability (Fig. 5).

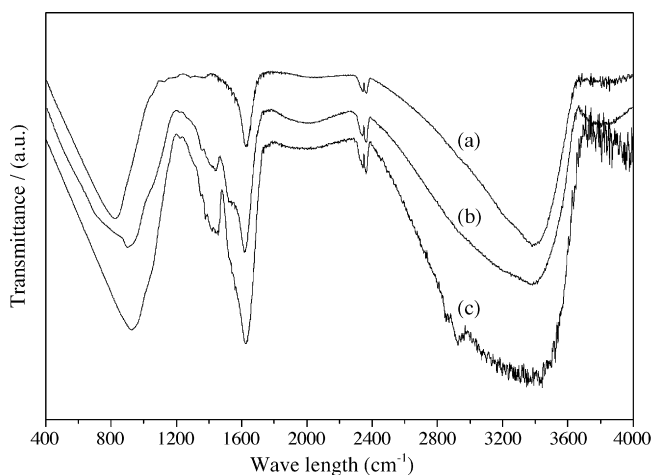


Fig. 3. The FT-IR spectra of (a) the as-prepared sample, (b) the sample heated at 400 °C for 3 h, and (c) the sample treated with ultrasonic.

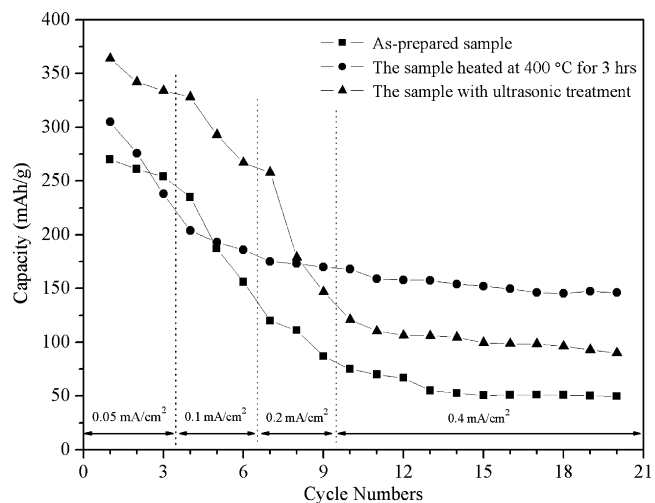


Fig. 5. Cyclabilities of the samples at various current densities of 0.05 mA cm⁻² during the 1st–3rd cycles, 0.1 mA cm⁻² during the 4th–6th cycles, 0.2 mA cm⁻² during the 7th–9th cycles, and 0.4 mA cm⁻² during the 10th–20th cycles.

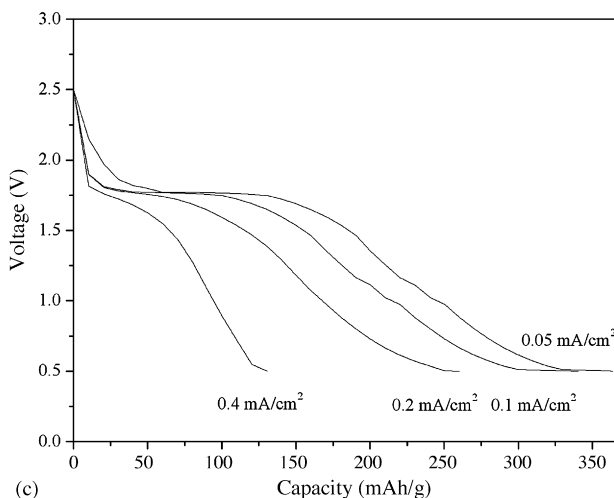
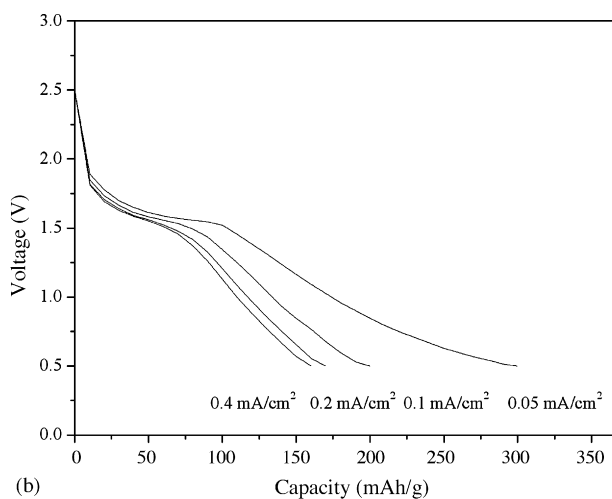
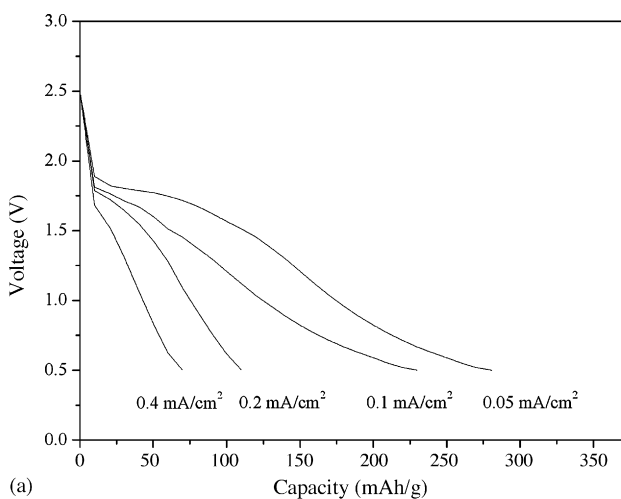


Fig. 4. The initial discharge profiles of (a) as-prepared sample, (b) the sample heated at 400 °C for 3 h, and (c) the sample with ultrasonic treatment at various current densities.

4. Conclusion

Nanocrystalline TiO₂ samples were prepared from the ethanol solution of titanium isopropoxide (Ti(O-*i*Pr)₄) and H₂O₂ at 80 °C for 48 h by refluxing method. We have investigated effect of heating and ultrasonic treatments. These treatments affected the electrochemical properties and morphology. All samples of the X-ray diffraction peaks are assigned to anatase phase TiO₂. The sample heated at 400 °C for 3 h shows the average crystalline size of 10 nm. Nanocrystalline TiO₂ prepared by treating with ultrasonic has monodispersed high aspect ratio particle shape morphology of a diameter of 5 nm and a length of 20 nm, when comparing with other samples. The sample treated with ultrasonic shows a good initial capacity with 340 mAh g⁻¹ at current density 0.05 mA cm⁻² in the voltage range of 2.5–0.5 V. However, its rate capability was worse than the sample heated at 400 °C for 3 h, indicating that a smaller particle size with spherical morphology provides a better rate capability. Further studies are needed on the optimization of processing conditions and are being carried out for high energy and high power applications.

Acknowledgements

This research was supported by the Program for the Training of Graduate Students in Regional Innovation which was con-

ducted by the Ministry of Commerce, Industry and Energy of the Korean Government.

References

- [1] K.M. Abraham, *Electrochim. Acta* 38 (1993) 1233.
- [2] S. Yamada, M. Fuliwara, M. Kanda, *J. Power Sources* 54 (1994) 209.
- [3] P. Fragnud, R. Nagarajan, D.M. Schleich, D. Vujic, *J. Power Sources* 54 (1995) 362.
- [4] Y. Gao, J.R. Dahn, *J. Electrochem. Soc.* 143 (1996) 100.
- [5] M. Ugaji, M. Hibino, T. Kudo, *J. Electrochem. Soc.* 142 (1995) 3664.
- [6] J.J. Auborn, Y.L. Barbero, *J. Electrochem. Soc.* 134 (1987) 368.
- [7] E. Ferg, J. Gummow, A. de Kock, M.M. Tackeray, *J. Electrochem. Soc.* 141 (1994) 147.
- [8] S.Y. Huang, L. Kavan, I. Exnar, M. Gratzel, *J. Electrochem. Soc.* 142 (1995) 142.
- [9] P. Poizot, S. Laruelle, S. Grugeon, L. Dupont, J.-M. Tarascon, *Nature* 407 (2000) 496.
- [10] C. Natarajan, K. Setoguchi, G. Nogami, *Electrochim. Acta* 43 (1998) 3371.
- [11] M. Hibino, K. Abe, M. Mochizuki, M. Miyayama, *J. Power Sources* 126 (2004) 139.
- [12] Y. Zhou, L. Cao, F. Zhang, B. He, H. Li, *J. Electrochem. Soc.* 150 (2003) 1246.
- [13] D. Peramunage, K.M. Abraham, *J. Electrochem. Soc.* 145 (1998) 2609.
- [14] D. Peramunage, K.M. Abraham, *J. Electrochem. Soc.* 145 (1998) 2615.